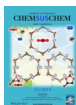


VIP Very Important Paper



Tuning Expanded Pores in Metal–Organic Frameworks for Selective Capture and Catalytic Conversion of Carbon Dioxide

Wei Meng,^[a] Yongfei Zeng,^{*[b]} Zibin Liang,^[a] Wenhan Guo,^[a] Chenxu Zhi,^[c] Yingxiao Wu,^[c] Ruiqin Zhong,^[c] Chong Qu,^[a] and Ruqiang Zou^{*[a]}

Three Co-based isostructural MOF-74-III materials with expanded pores are synthesized, with varied extent of fused benzene rings onto sidechain of same-length ligands to finely tune the pore sizes to 2.6, 2.4, and 2.2 nm. Gas sorption results for these highly mesoporous materials show that alternately arranged fused benzene rings on one side of the ligand could serve as extra anchoring sites for CO₂ molecules with π – π interactions, conspicuously enhancing CO₂ uptake and CO₂/CH₄ and CO₂/N₂ selectivity; while more steric hindrance effect towards open Co^{II} sites were imposed by ligands flanked with fused benzene rings on both sides, compromising such extra-sites enhance-

ment. In the catalytic conversion of CO₂ with propylene oxide to form propylene carbonate, the as-synthesized MOF-74-III(Co) with desired properties of highly exposed and accessible open Co^{II} centers, large mesopore apertures and multi-interactive sites, demonstrated higher catalytic activity compared with other two MOFs, with benzene rings fused to ligands hampering the functionality of Co^{II} centers as Lewis acid sites. Our results highlight the viability of finely tuning the expanded pores of MOF-74 isostructure and the effect of fused benzene rings as functional groups onto selective CO₂ capture and conversion.

Introduction

Metal–organic frameworks (MOFs)—a class of inorganic–organic hybrid crystalline materials—have sparked much interest among researchers, owing to their high surface areas, ordered porous structures, and the versatile tunability of their pore environments and functionalities, all of which could be implemented by judicious selection of various building blocks for synthesis by self-assembly,^[1] combined optionally with appropriate post-synthetic modifications.^[2] Generally, metal ions or clusters act as inorganic nodes, linked by organic bridging ligands containing elements such as oxygen, nitrogen, or sulfur. The highly desirable properties make MOFs promising materials for a wide variety of applications, with excellent performances in gas sorption/separation,^[3] catalysis,^[4] luminescence,^[5] sensing,^[6] electrochemistry,^[7] and magnetism.^[8] Among the

above applications, MOFs for sorption-based separation have made the most progress,^[9] especially for selective CO₂ capture.^[10] To address the issue of climate change caused by increasing emissions of anthropogenic CO₂ into the atmosphere, carbon capture and storage (or sequestration; CCS) was proposed as a significant route to CO₂ mitigation.^[11] Great efforts have been made to develop more advanced solid adsorbents for CO₂ capture,^[12] in light to the easy operation conditions, low energy cost for regeneration, and large working capacity of MOFs. Given the intrinsic formation of unlimited metal–ligand combinations in MOFs, they have been known to incorporate diverse metal-coordinated clusters, open metal sites, and many types of functional groups and to allow facile chemical treatment to form composites, leading to easier design of targeted materials than for other traditional adsorbents, such as activated carbon, silica gel, and zeolites.

Among the many known types of MOF, the well-known MOF-74 family, composed of helical one-dimensional chains of edge-connected metal–oxygen octahedra bridged by 2,5-dihydroxy-1,4-benzenedicarboxylic acid or some analogue to further form honeycomb networks, has become one of the most explored materials for many advanced applications,^[13] because of these materials' intriguing structural features.^[14] Upon removal of solvent molecules at metal sites by heating under vacuum, the coordination mode could be altered from octahedral to square pyramidal, leaving high-density open metal sites lining the channel inside.^[15] These materials show excellent potential as platforms with Lewis acid sites for gas sorption,^[16] catalysis,^[17] or post-synthetic grafting positions of functional species.^[18] Previous studies have demonstrated exceptionally

[a] W. Meng, Z. Liang, W. Guo, C. Qu, Prof. Dr. R. Zou
Beijing Key Laboratory for Theory and Technology of Advanced Battery Materials, Department of Materials Science and Engineering
College of Engineering, Peking University, Beijing 100871 (China)
E-mail: rzou@pku.edu.cn

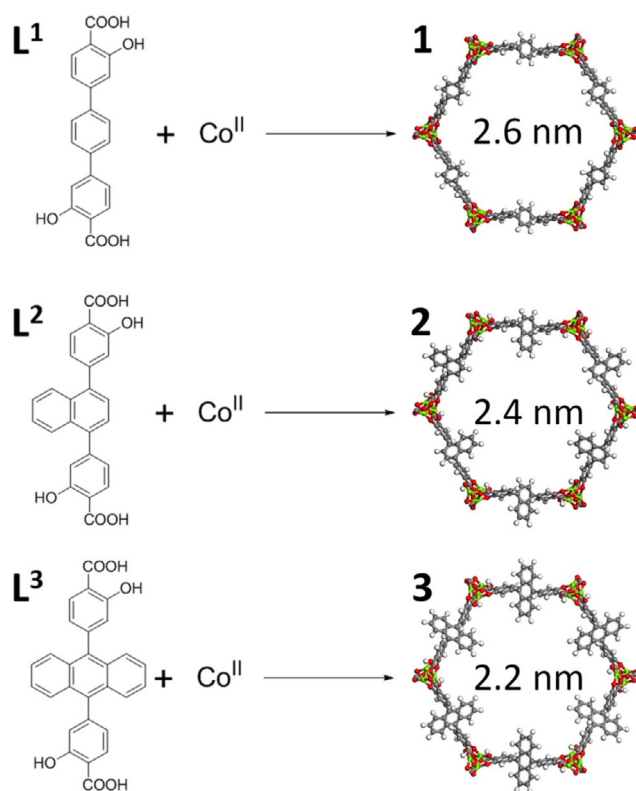
[b] Prof. Dr. Y. Zeng
Tianjin Key Laboratory of Structure and Performance for Functional Molecules, Key Laboratory of Inorganic–Organic Hybrid Functional Material Chemistry (Ministry of Education)
College of Chemistry, Tianjin Normal University, Tianjin 300387 (China)
E-mail: yfzeng@nankai.edu.cn

[c] C. Zhi, Y. Wu, Prof. Dr. R. Zhong
State Key Laboratory of Heavy Oil Processing
China University of Petroleum, Beijing 102249 (China)

 Supporting information and the ORCID identification number(s) for the author(s) of this article can be found under:
<https://doi.org/10.1002/cssc.201801585>.

high CO₂ adsorption of Mg-MOF-74 with open Mg^{II} sites at a concentration of more than 8 mmol g⁻¹ at 298 K and 1 bar,^[19] and amine-appended derivatives have shown even better tunability for CO₂ capture under different conditions.^[18,20] Furthermore, the unexpected mechanism of CO₂ interaction was verified by comprehensive experimental analysis.^[21] Recent works have structurally resolved some of the sorption sites and dynamics of CO₂ with frameworks.^[20d,22] However, although systematic expansion of MOF-74 pores has already been reported,^[14b] along with some examples with functional amine groups,^[20a,23] little work has been focused on strategies to finely tune pore size in expanded MOF-74 isostructures.

Herein, for the first time, we have employed the ligand 3,3'-dihydroxy-[1,1':4',1''-terphenyl]-4,4''-dicarboxylic acid (denoted as L¹) and another two analogues with different polyacenes as the middle strut, incorporating different numbers of fused benzene rings (Scheme 1, L² and L³), together with Co^{II} cations to construct MOFs with IRMOF-74-III structure featuring finely tuned pores. We then carefully examined their selective CO₂ capture and conversion performance to unravel the pore-size tuning effect brought about by sidechain fused benzene rings. This also exemplifies a Co-based expanded-pore MOF-74, with the fascinating electronic configuration of Co²⁺, compared with Mg²⁺, Zn²⁺ and Ni²⁺, to help elucidate its intrinsic effect on Lewis acidity-related applications.



Scheme 1. Synthesis of Co-based MOF-74-III materials **1**, **2**, and **3** (gray = C, red = O, olive = Co, white = H).

Results and Discussion

Characterization of MOF-74-III(Co) materials

The as-synthesized MOF-74-III(Co) materials were obtained through one-pot solvothermal synthesis, and the crystallinity is confirmed by the powder X-ray diffraction (PXRD) patterns (see the Supporting Information, Figure S1). The patterns of all three products matched well with reported simulated values,^[14b] with no undesired peaks, indicating the high purity of the materials. Taking account of the size of fused benzene ring(s) that form the polycyclic part of ligands along with the reported structure,^[14b,20a] the pore sizes of MOF-74-III(Co) materials can be presumably deduced as 2.6, 2.4, and 2.2 nm for **1**, **2**, and **3** (Scheme 1) respectively. From N₂ sorption measurements (Figure 1), each of the three activated materials demonstrates a type IV isotherm, which is typical of mesoporous materials.^[24] At $P/P_0 < 0.003$, the isotherms exhibit steep uptake, followed by a second uptake step at $P/P_0 = 0.05\text{--}0.14$, after which a plateau is reached. The isotherms of MOF-74-III(Co) species **1** and **2** both have distinct two-step profiles, whereas in that for **3**, the two steps are connected by an almost smooth transition, making the distinction between the steps unclear and more like a continuous pore filling, as is seemingly characteristic of micropores. Since monolayer–multilayer adsorbed N₂ occupied the narrow mesopore space, this altered the effective potential for pore filling.^[25] The evolution of the isotherm profiles and the shift of the second step position (with starting points at $P/P_0 = 0.11$, 0.068, and 0.048 for **1**, **2**, and **3**, respectively) reflect well the trend in pore size tuning. Moreover, the DFT fitting-derived pore size distributions further validate the pore apertures of MOF-74-III(Co) materials as 2.6, 2.4, and 2.2 nm, showing single peaks (Figure 1, inset). The second steps of the three isotherms, which are due to pore condensation, are accompanied by fully reversible desorption branches with no hysteresis, providing further evidence for the narrow mesopores of these materials. The BET surface areas of MOF-74-III(Co) are calculated as 2941, 2712, and 2065 m² g⁻¹, and the pore volumes are 1.77, 1.38, and 1.15 cm³ g⁻¹ for **1**, **2**, and **3**, respectively (Table S1). The morphology of each sample was observed with TEM to be one-dimensional rod-like microcrystalline particles (Figure S2). To test the stability, thermogravimetric analysis of the materials showed that desolvation occurred upon initial heating until 140–160 °C, after which the frameworks lost no weight up to about 260–280 °C, indicating the thermal stability of the materials (Figure S3).

Gas sorption by MOF-74-III(Co) materials

These highly porous structures with exposed Co^{II} sites may endow the materials with excellent potential for gas uptake. We performed gas sorption tests on **1**, **2**, and **3** with ultrahigh purity CO₂, CH₄, and N₂. From the obtained isotherms, all the materials present selective capture of CO₂ over CH₄ and N₂. As shown in Figure 2a, **1** demonstrates CO₂ uptake of 101.0 cm³ g⁻¹ at 273 K and 1 bar, and 75.1 cm³ g⁻¹ at 298 K and 1 bar, with selectivities for CO₂/N₂ mixtures (CO₂/N₂ = 15:85 v/v)

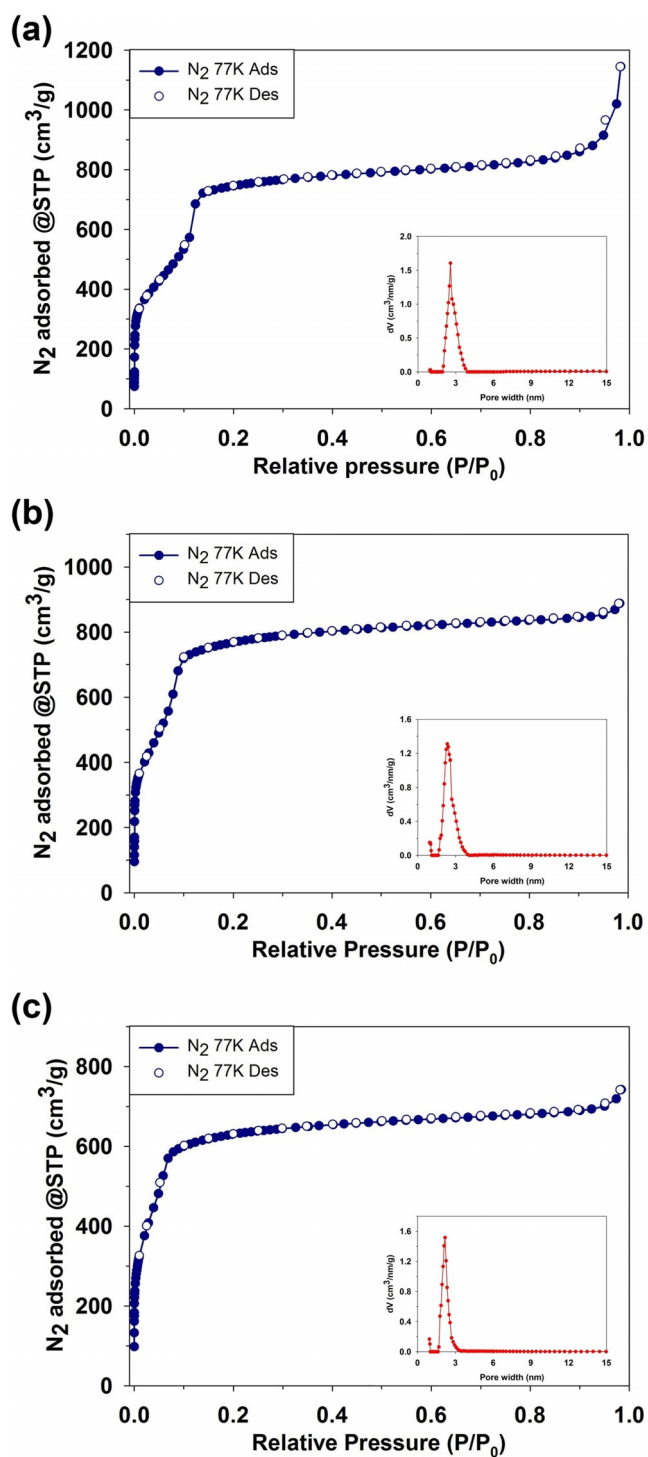


Figure 1. Nitrogen adsorption–desorption isotherms at 77 K and pore size distributions of MOF-74-III(Co) materials 1 (a), 2 (b), and 3 (c).

as high as 60.4 at 273 K and 35.9 at 298 K (calculated by IAST method; Figures S4 and S5). In addition, the isosteric heat of adsorption (Q_{st}) for CO_2 was calculated based on the isotherms of 273 and 298 K by using the Clausius–Clapeyron equation.^[26] Similar sorption enthalpies and trends with increasing CO_2 uptake indicate that these three materials have comparable affinities towards CO_2 with only slight differences (Figure S6).

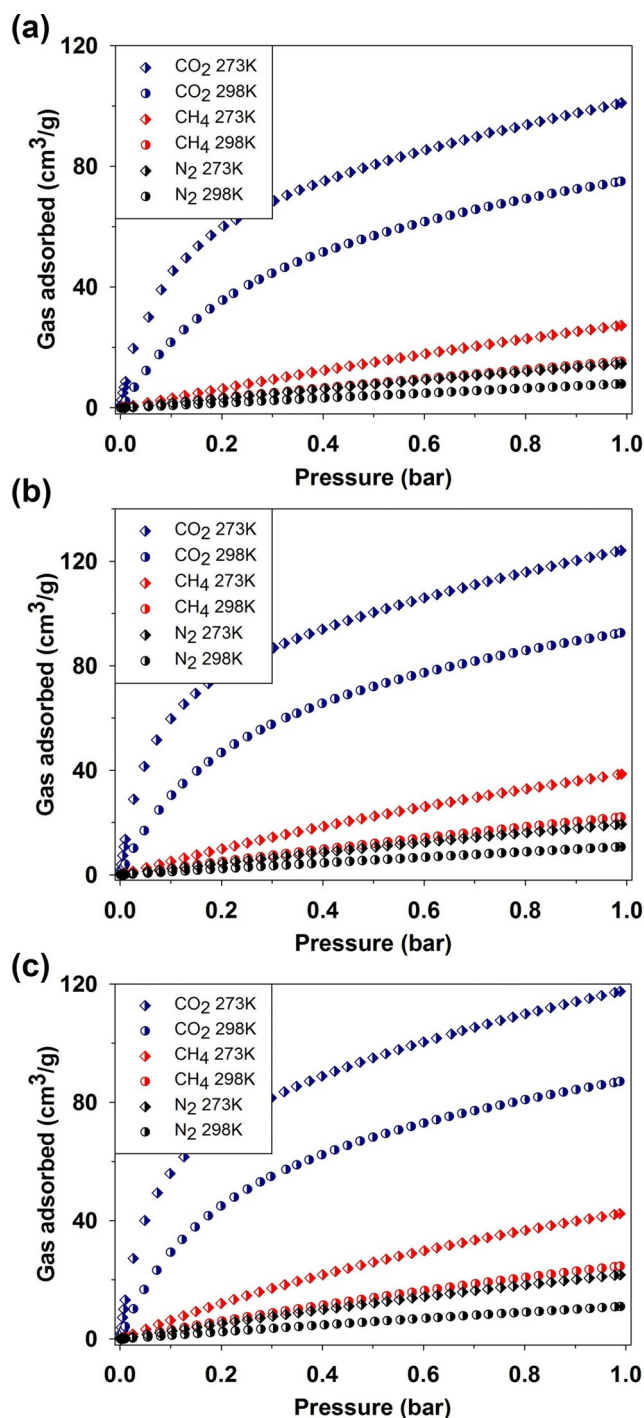


Figure 2. CO_2 , CH_4 , and N_2 adsorption isotherms at 273 and 298 K for MOF-74-III(Co) materials 1 (a), 2 (b), and 3 (c).

This could be attributed to the same open Co^{II} sites acting as Lewis acids to interact with CO_2 , along with fused benzene rings to impact weak π – π forces to synergistically attract gas molecules. From the Q_{st} curves, all materials demonstrate close initial enthalpy values (ca. -34 $kJ\ mol^{-1}$), indicating the affinity of open Co^{II} centers towards CO_2 , corresponding well with previous reports.^[19a] Additionally, the gradual decrease in Q_{st} leads to differences in binding strength of various sorption sites.

Benzene rings fused to the linkers of the framework have various effects on the properties of materials **1**, **2**, and **3**. The expanded π aromatic rings could affect local electronic environments and could also be regarded as “pore-size tuners”, additionally bringing about steric hindrance around Co^{II} sites. Furthermore, the increased mass density of the framework with no significant alteration in cell volume challenged some of evaluation concepts, taking into account that isostructural MOF-74-III materials retain very close crystalline cell parameters.

Indeed, through comparison of CO_2 sorption among the three materials, one could understand more about the effect of fused benzene rings on the framework. The CO_2 sorption isotherms of **1**, **2**, and **3** at 273 K and 298 K (Figure 3a and S7a in Supporting Information, respectively) were generally measured and normalized by the unit of cm^3g^{-1} as gravimetric uptake, and the highest adsorption was achieved by **2**. However, the enhanced CO_2 uptake of **3** was compromised by its increased framework weight, which is accounted for in the evaluation unit. If the crystalline unit-cell mass density is considered, the derived isotherms of volumetric uptake of the three

materials (Figure 3b and Figure S7b) demonstrate a more distinct regularity. From **1** to **2**, the volumetric uptake of CO_2 was drastically enhanced by 36.1% at 273 K (from 59.5 to 81.0 $\text{cm}^3\text{cm}^{-3}$) and 36.7% at 298 K (from 44.2 to 60.4 $\text{cm}^3\text{cm}^{-3}$). From **2** to **3** the uptake was also improved, albeit slightly, by 4.0% at 273 K (from 81.0 to 84.2 $\text{cm}^3\text{cm}^{-3}$) and 3.3% at 298 K (from 60.4 to 62.4 $\text{cm}^3\text{cm}^{-3}$). As is well known for isostructural materials of MOF-74, the coordinatively unsaturated metal (CUM) centers act as major sorption sites for various gas molecules, contributing mostly to the heat of adsorption,^[19a,22a,27] whereas the benzene rings fused to the framework should be considered as weakly polar functional groups, attracting CO_2 synergistically. According to previous reports,^[22a,b,28] CO_2 adsorbed onto MOF-74 materials can populate three kinds of sorption sites; the CUM centers are occupied first, followed by the neighboring carboxylate groups to form weak interactions, with the third CO_2 binding site located close to the center of the one-dimensional pore channel. In our case, besides these three sites, the fused benzene rings on the ligands form atomically thin pore walls that could serve as extra anchoring positions for gas molecules through less-selective van der Waals forces.^[29] Hence the volumetric uptake of CO_2 from **1** to **2** to **3** was successively enhanced. However owing to steric effects, the ligands of **3** flanked with benzene rings on both sides hindered the accessibility of open Co^{II} centers as strong sorption sites, lessening the packing density of CO_2 molecules around the CUM centers.^[25] For **2**, the fused benzene rings were oriented alternately towards the center of the channel, causing less steric hindrance and space occupation. These two competing factors resulted in much-enhanced (volumetric) CO_2 uptake of **2** compared to **1**, whereas CO_2 uptake in **3**, even with decreased gravimetric uptake, was slightly enhanced compared to that in **2**.

Notably, the CO_2 sorption performance of materials **1**, **2**, and **3** should be mostly attributed to the much stronger affinity of CUM sites towards CO_2 molecules compared to other binding sites. However, for CH_4 and N_2 , the uptake is very different. The uptake of CH_4 and N_2 at 273 K and 298 K was evidently improved from **1** to **2** to **3** (Figures S8 and S9), both gravimetrically and volumetrically,^[30] since weak adsorbate–pore wall interactions are present at every possible binding site. From the derived Q_{st} data (Figure S10), physical sorption could be inferred. Therefore, for CH_4 and N_2 the increased density of sorption sites combined with diminished influence on site occupancies imposed by steric factors of functional groups contributed to a clear and regular increased uptake of CH_4 and N_2 from **1** to **2** to **3**.

CO_2 fixation with epoxides catalyzed by MOF-74-III(Co) materials

Besides selective sorption of CO_2 with as-synthesized MOFs to address the issue of CCS, an alternative means of mitigating carbon-emission is to chemically convert CO_2 into value-added products. Among various transformations, the cycloaddition reaction between CO_2 and epoxides is one of the most efficient methods,^[31] producing cyclic organic carbonates, which are

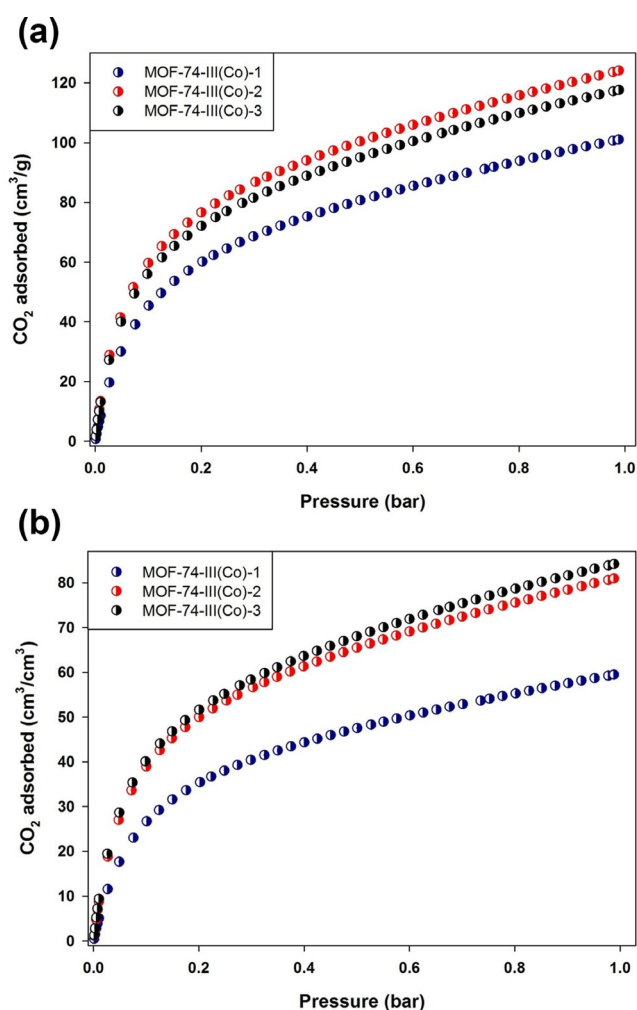
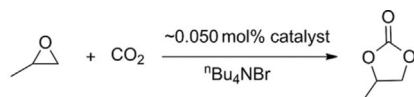


Figure 3. Isotherms of CO_2 adsorption at 273 K for **1**, **2**, and **3**. Gravimetric capacity (a) and volumetric capacity (b) are plotted together for comparison.

widely used in the pharmaceutical and chemical industries. MOF-based heterogeneous catalysts for this reaction have gained much attention,^[32] since Lewis acid sites are abundant in some MOF structures. Moreover, in some recent developments, cationic groups were incorporated in porous materials to build multifunctional catalysts without need for cocatalysts, such as imidazolium-functionalized frameworks.^[33] In our MOF-74-III(Co) materials, the unsaturated Co^{II} centers, highly mesoporous structure, and multiple active sites make **1**, **2**, and **3** promising candidates for such applications. Therefore, the catalytic performances of **1**, **2**, and **3** in the cycloaddition of CO₂ with propylene oxide into propylene carbonate (Scheme 2)



Scheme 2. Catalytic cycloaddition of CO₂ with propylene oxide to produce propylene carbonate.

was explored. The reactions catalyzed by **1**, **2**, and **3** from propylene oxide gave yields of 98, 88, and 51 %, respectively, with corresponding turnover frequencies (TOFs) 41, 37, and 21 h⁻¹ per Co^{II} center (at first cycle; Figure 4 and Table S2). The results clearly demonstrate that the catalytic activity decreases in the order **1** > **2** > **3** and that **1** shows especially high performance for catalytic cycloaddition. Recycled catalysts collected by centrifugation were then further investigated in the following two cycles, with analysis showing no significant decrease in catalytic activity for all three materials.

The remarkably higher performance of material **1** in this catalysis compared to **2** and **3** at the same condition, should be ascribed to the more accessible CUM centers as quite active Lewis acid sites, while for **2** and **3** the linkers flanked with ben-

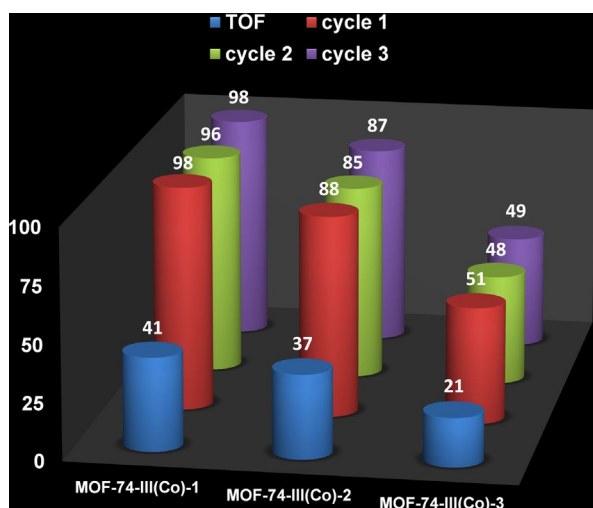


Figure 4. Yields (%) and TOFs (h⁻¹) for the cycloaddition of CO₂ and propylene oxide to propylene carbonate with different MOF catalysts for up to three cycles. TOF was calculated by moles of propylene carbonate yielded/ moles of catalyst based on open metal sites and reaction time.

zene rings have sterically hindered the attaching of substrate propylene oxide molecules, according to proposed catalytic mechanism.^[34] Moreover, the significantly weakened activity of **3** compared to **2** also indicates that dual side-fused benzene rings could impose more hindrance to open Co^{II} centers, whereas one side-fused rings, as in **2**, could be arranged alternately towards the inside channel, consistent with the results of gas uptake. The adverse steric effect could also hamper the kinetic diffusion of reactants and/or intermediates, further affecting the performance in catalysis.

The recyclability of **1**, **2**, and **3** as heterogeneous catalysts, as indicated by the maintained catalytic activity in three successive cycles of the reaction, could be further investigated by obtaining powder XRD patterns after recycling (Figure S11). In comparison with the simulated patterns, no undesired peaks were observed. The well-retained crystallinity indicated superior stability through catalytic cycles. Therefore, by utilizing a high density of CUM centers and mesoporous structure of **1**, we acquired high performance in catalytic activity and good reusability in CO₂ fixation with propylene oxide, making it an excellent candidate as a heterogeneous catalyst. While the comparison of **2** and **3** with **1**, has for the first time unravelled the effect of fused benzene rings to the performance of framework.

Conclusions

In summary, we have synthesized expanded-pore MOF-74-III(Co) materials **1**, **2**, and **3**, with pore sizes tuned to 2.6, 2.4, and 2.2 nm, respectively. With the fused benzene rings incorporated within the ligands, not only the channel apertures, but also chemical environment of pore walls were finely altered. Owing to the nonselective van der Waals interactions introduced by the benzene rings, gas sorption was enhanced with respect to CO₂, CH₄, and N₂. However, owing to steric hindrance imposed by linkers L³ on the open Co^{II} sites, the strong affinity of CUM centers towards CO₂ was drastically affected, leading to slightly improved volumetric CO₂ uptake (and decreased gravimetric uptake) of **3** compared to **2**. Therefore, the MOF-74-III(Co)-2 showed the highest selectivity among the three materials for CO₂/CH₄ and CO₂/N₂ sorption-based separation. Furthermore, in testing the catalytic activities of **1**, **2**, and **3** for CO₂ cycloaddition with propylene oxide, **1** showed the best activity, owing to highly exposed CUM centers, large mesopore apertures, and multiple active sites for efficient access and activation of epoxides at the Lewis acid sites, along with readily diffusive pathways and synergistic affinity to CO₂. For **2** and **3**, the steric effect of benzene-fused linkers hampered the spatial availability of open Co^{II} sites, lowering the catalytic activity to some extent. Our results have elucidated the effect of fused benzene rings incorporate within ligands on the properties and performances of materials **1**, **2**, and **3**, and shown that cobalt based MOF-74-III materials could be very promising candidates for CO₂-related sorption, separation, and catalysis applications, upon finely tuning the linkers. Investigations into the moisture stability of these materials and their modification with amines, which could effectively take advantage of the ex-

panded-pore framework as a potential multifunctional platform, are currently underway.

Experimental Section

Synthesis of MOF-74-III(Co)

Ligands L¹, L², and L³ were prepared by coupling reactions (see the Supporting Information). The MOF-74-III materials were synthesized under solvothermal conditions according to a previously reported method^[14b] with slight modifications. Typically, Co(NO₃)₂·6H₂O (180 mg, 0.62 mmol) and the organic ligand (0.188 mmol) were mixed and dissolved in *N,N*-dimethylformamide (DMF; 15 mL). After sonication for 10 min, ethanol (1.0 mL) followed by deionized water (1.0 mL) were added to the solution. The mixture was sonicated again for 10 min, then placed in a Teflon-lined stainless-steel autoclave and heated at 120 °C for 24 h. The system was then allowed to cool to room temperature. The obtained material was collected and soaked first in DMF (20 mL) then in methanol (20 mL) three times, while solvents were replaced every 12 h. The final products were filtered and activated under vacuum at 200 °C for 12 h. The products were denoted as MOF-74-III(Co)-1, 2, and 3, corresponding to ligands L¹, L², and L³, respectively.

Characterization

Powder X-ray diffraction patterns were collected on a Rigaku SmartLab 9 kW diffractometer using Cu_{Kα} radiation ($\lambda = 1.5406 \text{ \AA}$), operating at 45 kV and 200 mA. Thermogravimetric analyses were carried out on a TA Instruments SDT Q600 analyzer with a heating rate of 10 °C min⁻¹ under nitrogen flow (100 mL min⁻¹). Transmission electron microscopy (TEM) images were obtained by using a FEI Tecnai F20 microscope.

Gas sorption measurements

The sorption isotherms were recorded with a Quantachrome Autosorb-iQ gas adsorption analyzer. The as-synthesized sample (ca. 100 mg) was placed in the sample tube and degassed at 200 °C for 6 h to remove the solvent molecules prior to the measurements. Ultrahigh-purity (99.999%) N₂, CO₂, and CH₄ were used for all measurements. The temperatures were controlled by using a liquid-nitrogen bath (77 K) or a glycol–water cycling bath (273 and 298 K). The Brunauer–Emmett–Teller (BET) surface areas were calculated from the adsorption branches. Pore size distributions (PSDs) were fitted with Non-Local Density Functional Theory (NLDFT) using the model of cylindrical pores.

Catalysis experiments

In a typical reaction, a test tube was charged with propylene oxide (40 mmol), catalyst (0.02 mmol, 0.05 mol% calculated based on open metal sites, pre-activated by vacuum drying at 200 °C for 6 h) and cocatalyst of *tert*-butylammonium bromide (TBAB, 1.5 mmol), which was placed into a 600 mL Parr reactor. The reactor was slowly pressurized to 12 bar with CO₂ and maintained at room temperature (ca. 23 °C) under stirring for 48 h. The reactor was depressurized and the products were monitored by GC (HP-5MS column) with *n*-dodecane as an internal standard. Only propylene carbonate was identified by comparison of the peak area to the internal standard from GC, which was utilized to calculate the yield of propylene oxide. The catalyst was recovered by centrifuge for

the next cycle and washed with methanol (3×10 mL). The process was repeated by using the recovered catalyst, which had been dried under vacuum at 200 °C for 6 h.

Acknowledgements

This work is funded by the Peking University CCUS project supported by BHP Billiton, the Natural Science Foundation of China (51772008, 21771138), National Program for Support of Top-notch Young Professionals, Changjiang Scholar Program, and the program of Thousand Youth Talents in Tianjin of China.

Conflict of interest

The authors declare no conflict of interest.

Keywords: adsorption · CO₂ fixation · gas separation · heterogeneous catalysis · metal–organic frameworks

- [1] a) H. Furukawa, K. E. Cordova, M. O’Keeffe, O. M. Yaghi, *Science* **2013**, *341*, 1230444; b) V. Guillerm, D. Kim, J. F. Eubank, R. Luebke, X. Liu, K. Adil, M. S. Lah, M. Eddaoudi, *Chem. Soc. Rev.* **2014**, *43*, 6141–6172; c) W. Lu, Z. Wei, Z. Y. Gu, T. F. Liu, J. Park, J. Park, J. Tian, M. Zhang, Q. Zhang, T. Gentle, 3rd, M. Bosch, H. C. Zhou, *Chem. Soc. Rev.* **2014**, *43*, 5561–5593.
- [2] a) S. M. Cohen, *J. Am. Chem. Soc.* **2017**, *139*, 2855–2863; b) S. M. Cohen, *Chem. Rev.* **2012**, *112*, 970–1000.
- [3] a) L. Kong, R. Zou, W. Bi, R. Zhong, W. Mu, J. Liu, R. P. S. Han, R. Zou, *J. Mater. Chem. A* **2014**, *2*, 17771–17778; b) J. Liu, W. Xia, W. Mu, P. Li, Y. Zhao, R. Zou, *J. Mater. Chem. A* **2015**, *3*, 5275–5279; c) J. Liu, Y. Wei, P. Li, Y. Zhao, R. Zou, *J. Phys. Chem. C* **2017**, *121*, 13249–13255.
- [4] a) X. Han, X.-J. Wang, P.-Z. Li, R. Zou, M. Li, Y. Zhao, *CrystEngComm* **2015**, *17*, 8596–8601; b) P. Z. Li, X. J. Wang, J. Liu, J. S. Lim, R. Zou, Y. Zhao, *J. Am. Chem. Soc.* **2016**, *138*, 2142–2145; c) R. Zou, P. Z. Li, Y. F. Zeng, J. Liu, R. Zhao, H. Duan, Z. Luo, J. G. Wang, R. Zou, Y. Zhao, *Small* **2016**, *12*, 2334–2343; d) J. Liang, Z. Liang, R. Zou, Y. Zhao, *Adv. Mater.* **2017**, *29*, 1701139.
- [5] a) S. S. Nagarkar, A. V. Desai, S. K. Ghosh, *Chem. Eur. J.* **2015**, *21*, 9994–9997; b) Z. Hu, B. J. Deibert, J. Li, *Chem. Soc. Rev.* **2014**, *43*, 5815–5840.
- [6] a) D. J. Wales, J. Grand, V. P. Ting, R. D. Burke, K. J. Edler, C. R. Bowen, S. Mintova, A. D. Burrows, *Chem. Soc. Rev.* **2015**, *44*, 4290–4321; b) C. He, K. Lu, W. Lin, *J. Am. Chem. Soc.* **2014**, *136*, 12253–12256.
- [7] a) W. Xia, J. Zhu, W. Guo, L. An, D. Xia, R. Zou, *J. Mater. Chem. A* **2014**, *2*, 11606–11613; b) W. Xia, A. Mahmood, R. Zou, Q. Xu, *Energy Environ. Sci.* **2015**, *8*, 1837–1866; c) W. Xia, R. Zou, L. An, D. Xia, S. Guo, *Energy Environ. Sci.* **2015**, *8*, 568–576; d) Q. L. Zhu, W. Xia, T. Akita, R. Zou, Q. Xu, *Adv. Mater.* **2016**, *28*, 6391–6398; e) Z. Liang, W. Xia, C. Qu, B. Qiu, H. Tabassum, S. Gao, R. Zou, *ChemElectroChem* **2017**, *4*, 2442–2447; f) H. Tabassum, W. Guo, W. Meng, A. Mahmood, R. Zhao, Q. Wang, R. Zou, *Adv. Energy Mater.* **2017**, *7*, 1601671.
- [8] a) L. C. Gómez-Aguirre, B. Pato-Doldan, J. Mira, S. Castro-García, M. A. Senaris-Rodríguez, M. Sanchez-Andujar, J. Singleton, V. S. Zapf, *J. Am. Chem. Soc.* **2016**, *138*, 1122–1125; b) J. Vallejo, F. R. Fortea-Pérez, E. Pardo, S. Benmansour, I. Castro, J. Krzystek, D. Armentano, J. Cano, *Chem. Sci.* **2016**, *7*, 2286–2293.
- [9] a) J. R. Li, J. Sculley, H. C. Zhou, *Chem. Rev.* **2012**, *112*, 869–932; b) J. R. Li, R. J. Kuppler, H. C. Zhou, *Chem. Soc. Rev.* **2009**, *38*, 1477–1504.
- [10] a) E. González-Zamora, I. A. Ibarra, *Mater. Chem. Front.* **2017**, *1*, 1471–1484; b) Y. Lin, C. Kong, Q. Zhang, L. Chen, *Adv. Energy Mater.* **2017**, *7*, 1601296; c) J. Yu, L. H. Xie, J. R. Li, Y. Ma, J. M. Seminario, P. B. Balbuena, *Chem. Rev.* **2017**, *117*, 9674–9754; d) C. A. Trickett, A. Helal, B. A. Al-Maythaly, Z. H. Yamani, K. E. Cordova, O. M. Yaghi, *Nat. Rev. Mater.* **2017**, *2*, 17045.

- [11] a) J. D. Figueroa, T. Fout, S. Plasynski, H. McIlvried, R. D. Srivastava, *Int. J. Greenhouse Gas Control* **2008**, *2*, 9–20; b) R. S. Haszeldine, *Science* **2009**, *325*, 1647–1652.
- [12] a) Q. Wang, J. Luo, Z. Zhong, A. Borgna, *Energy Environ. Sci.* **2011**, *4*, 42–55; b) A. Samanta, A. Zhao, G. K. H. Shimizu, P. Sarkar, R. Gupta, *Ind. Eng. Chem. Res.* **2012**, *51*, 1438–1463.
- [13] a) B. Qiu, C. Yang, W. Guo, Y. Xu, Z. Liang, D. Ma, R. Zou, *J. Mater. Chem. A* **2017**, *5*, 8081–8086; b) C. Qu, B. Zhao, Y. Jiao, D. Chen, S. Dai, B. M. deglee, Y. Chen, K. S. Walton, R. Zou, M. Liu, *ACS Energy Lett.* **2017**, *2*, 1263–1269; c) C. Qu, L. Zhang, W. Meng, Z. Liang, B. Zhu, D. Dang, S. Dai, B. Zhao, H. Tabassum, S. Gao, H. Zhang, W. Guo, R. Zhao, X. Huang, M. Liu, R. Zou, *J. Mater. Chem. A* **2018**, *6*, 4003–4012.
- [14] a) N. L. Rosi, J. Kim, M. Eddaoudi, B. Chen, M. O’Keeffe, O. M. Yaghi, *J. Am. Chem. Soc.* **2005**, *127*, 1504–1518; b) H. Deng, S. Grunder, K. E. Cordova, C. Valente, H. Furukawa, M. Hmadeh, F. Gandara, A. C. Whalley, Z. Liu, S. Asahina, H. Kazumori, M. O’Keeffe, O. Terasaki, J. F. Stoddart, O. M. Yaghi, *Science* **2012**, *336*, 1018–1023.
- [15] P. D. Dietzel, R. E. Johnsen, R. Blom, H. Fjellvag, *Chem. Eur. J.* **2008**, *14*, 2389–2397.
- [16] P. D. Dietzel, B. Panella, M. Hirscher, R. Blom, H. Fjellvag, *Chem. Commun.* **2006**, *0*, 959–961.
- [17] H. Jiang, Q. Wang, H. Wang, Y. Chen, M. Zhang, *ACS Appl. Mater. Interfaces* **2016**, *8*, 26817–26826.
- [18] T. M. McDonald, W. R. Lee, J. A. Mason, B. M. Wiers, C. S. Hong, J. R. Long, *J. Am. Chem. Soc.* **2012**, *134*, 7056–7065.
- [19] a) S. R. Caskey, A. G. Wong-Foy, A. J. Matzger, *J. Am. Chem. Soc.* **2008**, *130*, 10870–10871; b) Z. Bao, L. Yu, Q. Ren, X. Lu, S. Deng, *J. Colloid Interface Sci.* **2011**, *353*, 549–556.
- [20] a) A. M. Fracaroli, H. Furukawa, M. Suzuki, M. Dodd, S. Okajima, F. Gandara, J. A. Reimer, O. M. Yaghi, *J. Am. Chem. Soc.* **2014**, *136*, 8863–8866; b) W. R. Lee, S. Y. Hwang, D. W. Ryu, K. S. Lim, S. S. Han, D. Moon, J. Choi, C. S. Hong, *Energy Environ. Sci.* **2014**, *7*, 744–751; c) P. Q. Liao, X. W. Chen, S. Y. Liu, X. Y. Li, Y. T. Xu, M. Tang, Z. Rui, H. Ji, J. P. Zhang, X. M. Chen, *Chem. Sci.* **2016**, *7*, 6528–6533; d) P. J. Milner, R. L. Siegelman, A. C. Forse, M. I. Gonzalez, T. Runcevski, J. D. Martell, J. A. Reimer, J. R. Long, *J. Am. Chem. Soc.* **2017**, *139*, 13541–13553; e) P. J. Milner, J. D. Martell, R. L. Siegelman, D. Gygi, S. C. Weston, J. R. Long, *Chem. Sci.* **2018**, *9*, 160–174.
- [21] T. M. McDonald, J. A. Mason, X. Kong, E. D. Bloch, D. Gygi, A. Dani, V. Crocella, F. Giordanino, S. O. Odoh, W. S. Drisdell, B. Vlasisavljevich, A. L. Dzubak, R. Poloni, S. K. Schnell, N. Planas, K. Lee, T. Pascal, L. F. Wan, D. Prendergast, J. B. Neaton, B. Smit, J. B. Kortright, L. Gagliardi, S. Bordiga, J. A. Reimer, J. R. Long, *Nature* **2015**, *519*, 303–308.
- [22] a) W. L. Queen, M. R. Hudson, E. D. Bloch, J. A. Mason, M. I. Gonzalez, J. S. Lee, D. Gygi, J. D. Howe, K. Lee, T. A. Darwish, M. James, V. K. Peterson, S. J. Teat, B. Smit, J. B. Neaton, J. R. Long, C. M. Brown, *Chem. Sci.* **2014**, *5*, 4569–4581; b) B. Pato-Doldán, M. H. Rosnes, P. D. C. Dietzel, *ChemSusChem* **2017**, *10*, 1710–1719; c) A. C. Forse, M. I. Gonzalez, R. L. Siegelman, V. J. Witherspoon, S. Jawahery, R. Mercado, P. J. Milner, J. D. Martell, B. Smit, B. Blumich, J. R. Long, J. A. Reimer, *J. Am. Chem. Soc.* **2018**, *140*, 1663–1673.
- [23] R. W. Flaig, T. M. Osborn Popp, A. M. Fracaroli, E. A. Kapustin, M. J. Kalmutzki, R. M. Altamimi, F. Fathieh, J. A. Reimer, O. M. Yaghi, *J. Am. Chem. Soc.* **2017**, *139*, 12125–12128.
- [24] K. A. Cychosz, R. Guillet-Nicolas, J. Garcia-Martinez, M. Thommes, *Chem. Soc. Rev.* **2017**, *46*, 389–414.
- [25] H. Sung Cho, H. Deng, K. Miyasaka, Z. Dong, M. Cho, A. V. Neimark, J. Ku Kang, O. M. Yaghi, O. Terasaki, *Nature* **2015**, *527*, 503–507.
- [26] R. L. Siegelman, T. M. McDonald, M. I. Gonzalez, J. D. Martell, P. J. Milner, J. A. Mason, A. H. Berger, A. S. Bhowan, J. R. Long, *J. Am. Chem. Soc.* **2017**, *139*, 10526–10538.
- [27] M. I. Gonzalez, J. A. Mason, E. D. Bloch, S. J. Teat, K. J. Gagnon, G. Y. Morrison, W. L. Queen, J. R. Long, *Chem. Sci.* **2017**, *8*, 4387–4398.
- [28] W. L. Queen, C. M. Brown, D. K. Britt, P. Zajdel, M. R. Hudson, O. M. Yaghi, *J. Phys. Chem. C* **2011**, *115*, 24915–24919.
- [29] R. A. Agarwal, N. K. Gupta, *Coord. Chem. Rev.* **2017**, *332*, 100–121.
- [30] T. M. McDonald, D. M. D’Alessandro, R. Krishna, J. R. Long, *Chem. Sci.* **2011**, *2*, 2022–2028.
- [31] H. He, J. A. Perman, G. Zhu, S. Ma, *Small* **2016**, *12*, 6309–6324.
- [32] a) J. Liang, Y.-B. Huang, R. Cao, *Coord. Chem. Rev.* **2017**, *351*, 189–204; b) M. Ding, H.-L. Jiang, *ACS Catal.* **2018**, *8*, 3194–3201; c) M. Ding, S. Chen, X. Q. Liu, L. B. Sun, J. Lu, H. L. Jiang, *ChemSusChem* **2017**, *10*, 1898–1903.
- [33] a) J. Liang, Y. Q. Xie, X. S. Wang, Q. Wang, T. T. Liu, Y. B. Huang, R. Cao, *Chem. Commun.* **2018**, *54*, 342–345; b) T. T. Liu, J. Liang, Y. B. Huang, R. Cao, *Chem. Commun.* **2016**, *52*, 13288–13291; c) J. Liang, R. P. Chen, X. Y. Wang, T. T. Liu, X. S. Wang, Y. B. Huang, R. Cao, *Chem. Sci.* **2017**, *8*, 1570–1575.
- [34] M. H. Beyzavi, C. J. Stephenson, Y. Liu, O. Karagiari, J. T. Hupp, O. K. Farha, *Front. Energy Res.* **2015**, *2*, 1–10.

 Manuscript received: July 13, 2018

Accepted manuscript online: August 20, 2018

Version of record online: October 22, 2018